2-2-2 Geospace Diagnostics by HF Radars

HORI Tomoaki

SuperDARN HF radars are powerful tools to diagnose large-scale plasma convection in the Geospace. Utilizing the King Salmon radar and the magnetometer chain data, we show that transient ionospheric flow shears appearing at sub-auroral latitudes in the dusk to evening sector are convection patterns caused by the transient imbalance between the Region-1 and Region-2 field-aligned currents.

Keywords
Ionospheric convection, Convection electric field, SuperDARN radar, Flow shear, Magnetometer

1 Introduction

1.1 Space weather research and international cooperation

The ceaseless pace of human expansion into outer space that began in the 1970s has resulted in several hundreds of communications, observatory and other kinds of artificial satellites coming into daily service, with international manned space stations hosting astronauts for many long months. Recent news of the incorporation of private space travel agencies remains fresh in our memory. Thus, the doors to outer space have been opened to general private citizens, as well selected groups of people, such as technicians and researchers. Amid mankind's growing dependence on outer space, the need for basic research on space weather phenomena and the related application of space weather prediction is expected to heighten.

With this background, space weather research has become a worldwide trend. The world's first space weather research began in 1988 by the Communications Research Laboratory (now the National Institute of Information and Communications Technology), with later research initiated by the United States of America as a national project in the 1990s. The European Space Agency (ESA) subsequently followed suit. More recently, frameworks for full-scale space weather research have also been built in such Asian nations as China and Korea, sparking intensive research. Plans have also been made to combine international research efforts. Among these efforts, CAWSES (Climate And Weather of the Sun-Earth System), a five-year program successfully carried out from 2004, has now evolved into a project called "CAWSES-II" since 2009 and is being driven by international joint research efforts like CAWSES on space weather.

1.2 Magnetosphere-ionosphere convections and the international SuperDARN project

Space weather is concerned with the far-reaching expanse of geospace extending from the terrestrial upper atmosphere (i.e., mesosphere, ionosphere, thermosphere) to near-earth outer space. Attempts to observe the variety of phenomena occurring in geospace essentially involve the international cooperation and international joint planning described above. One of these research projects is the international SuperDARN (Super Dual Auroral Radar Network) project[1]. In this project,

large high-frequency (HF) radars having the same set of functionality are installed in different parts of the globe, with observational data collected from these radars being shared across the international community to facilitate significant advances in space weather research. More than 20 radars are currently in service in the northern and southern hemispheres. Figure 1 shows the locations of the fields of view for SuperDARN radars erected in the northern hemisphere. Each SuperDARN radar site irradiates short-wave signals against the ionosphere and receives reflected echoes to measure plasma behavior in the F-layer of the ionosphere among other things. With an azimuth angle of 50° and a measuring range of 3000 km, the large field of view delivers a two-dimensional picture of the ionospheric plasma flow or so-called plasma convections.

Because ionospheric convections amount to an electric-field drift of ionospheric electrons, observing these convections provides insight into the convection electric field applied to the ionosphere. The dynamo source of this electric field is driven by interactions between the geomagnetosphere and solar winds, and brought into the ionosphere on field-aligned current. This means that measuring the electric field in the ionosphere as a huge screen will shed light on the convection structure of the entire magnetosphere as projected in the ionosphere along the field-aligned current. SuperDARN leverages a set of radars to perform network observations, thereby demonstrating its power to monitor the large-scale structure of these convections [2][3].

Extensive research has been directed at the large-scale structure of convections in the polar ionosphere, since it is believed to be an electronic projection of magnetospheric convections in the ionosphere. Prior to the 1980s, electric field observations from wide-area radars and extensive radars like those now being used had not been available, and many research efforts had exclusively derived an equivalent current system from data collected with magnetometers deployed worldwide and assumed that it is a hall current ($j \propto \vec{B} \times \vec{E}$) for the purpose of estimating an electrical potential structure. Nishida, et al. [4] demonstrated that the Disturbance of Polar Field 2 (DP2) current system consisted of two vortex structures as shown in Fig. 2. Nishida [5] went on to demonstrate that intensity fluctuations (DP2 fluctuations) in this current system had good correlations with fluctuations in the north-

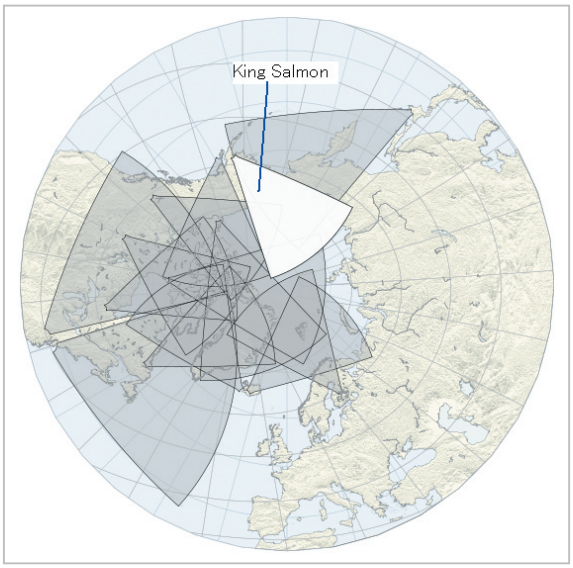

Fig.1 *SuperDARN radar fields of view in the northern hemisphere*

The sector denotes the field of view for each SuperDARN radar site.

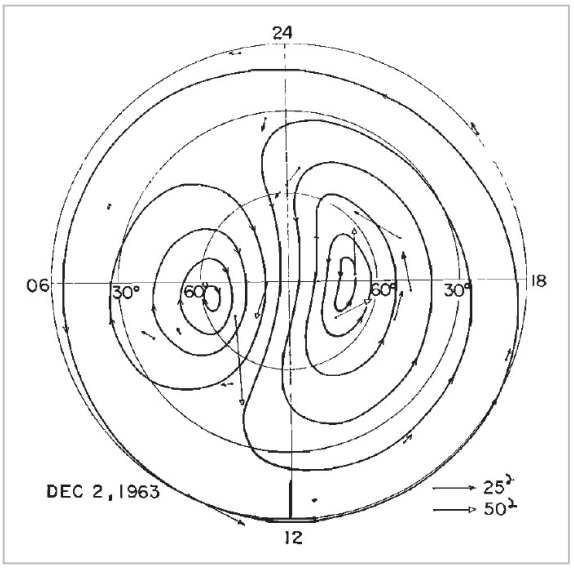

Fig.2 *DP2 current system identified from geomagnetic observations*

A dual-vortex structure reaching the lower latitudes

south component of the Interplanetary Magnetic Field (IMF).

Electric field observations by satellite and electric field drift observations of the ionospheric plasma flow have subsequently come into practice, offering insight into the large-scale convection structure of the ionosphere based on electric field observations. Figure 3 shows the average convection pattern resulting from statistical manipulations of SuperDARN observations. As shown in Fig. 3, the evening-side magnetic latitudes of 60 to 70° are associated with that part of the evening-side convection vortex returning from night to daytime, with westward ionospheric convections being normally dominant in this region.

Ionospheric convections are not always westward in this region, since an eastward plasma flow of convection opposite to the typical direction of convection is sometimes observed for a short interval of time. Because such an eastward plasma flow is often formed at lower latitudes than in the auroral region (normally 65° latitude or higher), a greater proportion of this flow often cannot be observed with existing SuperDARN radars having a field of view in the auroral region or on the higher-latitude side. Although this phenomenon is interesting, whether the eastward plasma flow is part of the global flow or is local has yet to be clarified.

Among all SuperDARN radars, the King Salmon radar operated by the National Institute of Information and Communications Technology can be considered optimally located to observe this phenomenon. In service since 2001 as part of SuperDARN, the King Salmon HF radar (KSR) can monitor the lowest-latitude range among existing SuperDARN radars, with the exception of a set of mid-latitude radars that recently came into service. Moreover, it is capable of directly measuring ionospheric plasma flow in the east-west direction as a Doppler velocity, because its radar beam is directed almost westward in the auroral and subauroral regions. Such transient eastward convections have been often observed by the KSR. The KSR has also spotted many instances of east-west flow shears (structure with adjoining reverse plasma flow)

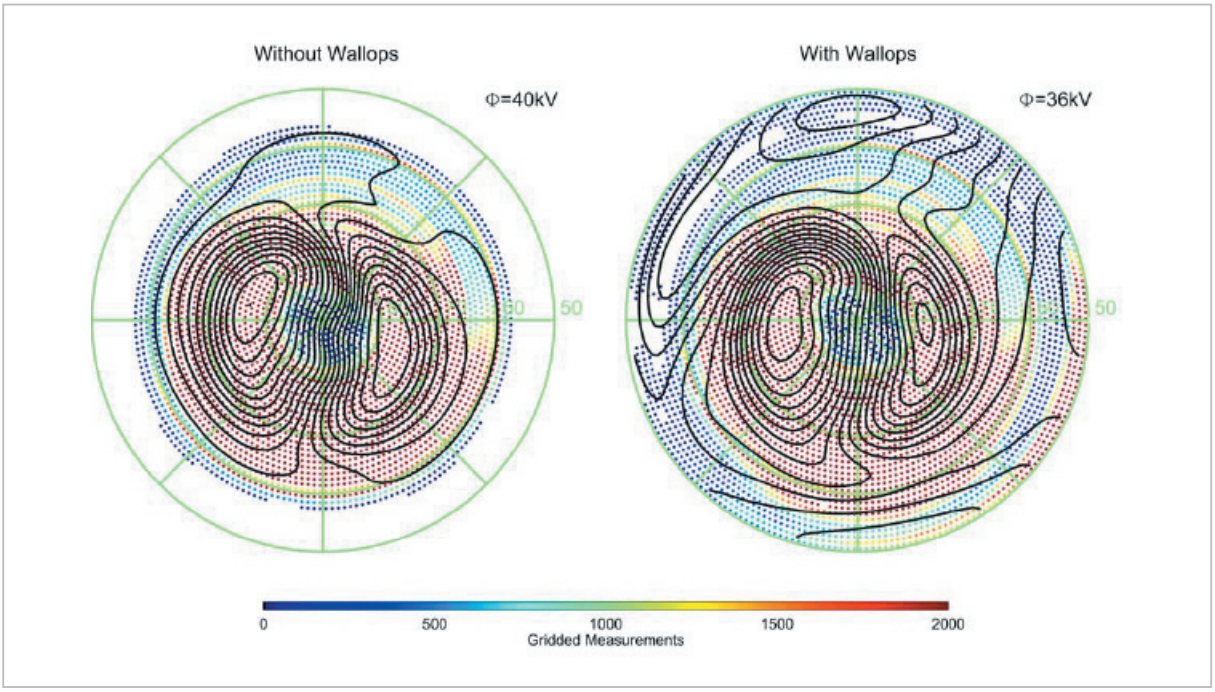

Fig.3 *Average convection pattern determined from SuperDARN observations*

The left and right diagrams denote results not including and including of mid-latitude observation data derived from Wallops radar, respectively.

involving westward convections opposite the eastward convections on the high-latitude side. The NICT-SWM (Space Weather Monitoring) magnetometers and RapidMag magnetometers (http://kogma.nict.go.jp/cgi-bin/geomag-interface/) also deployed by the National Institute of Information and Communications Technology are in service in the latitude and longitude bands covered by the KSR to measure broad ranges of geomagnetic fluctuations, and available for implementing multi-phased research using radar and a set of magnetometers [6]. Research has been conducted by leveraging these enhanced research resources with regard to the characteristics and mechanism of occurrence of flow shears accompanied by eastward convections appearing on the low-latitude side, with the aid of ground and satellite observations. This paper reports the findings of this research.

2 Case study

An example of eastward convections observed by the King Salmon radar in the latitude zone of normal westward convections is presented here. Figure 4 shows the field of view (inside the sector shown in the diagram) of the KSR at 09:00 UT on August 10, 2007, along with the locations of the RapidMag magnetometers (PBK, TIK, NOK, AMD) and NICT-SWM magnetometers (KSM, STC, PTK) (orange points in the diagram). RapidMag magnetometers are located to monitor intensity fluctuations (corresponding to intensity fluctuations in large-scale convections) of the DP2 current system, since they cover the auroral region over a wide range of local times in the afternoon. In contrast, the KSR has a field of view split into 16 beams (beams 00 to 15) in the arc direction of the sector, with each beam being further split into 75 range gates in the radial direction. Since it normally takes two minutes for a full field of view scan, the horizontal velocity field of plasma in the F-layer of the ionosphere can be obtained every two minutes. In particular, beam 02 (marked by a red line) passes almost directly above

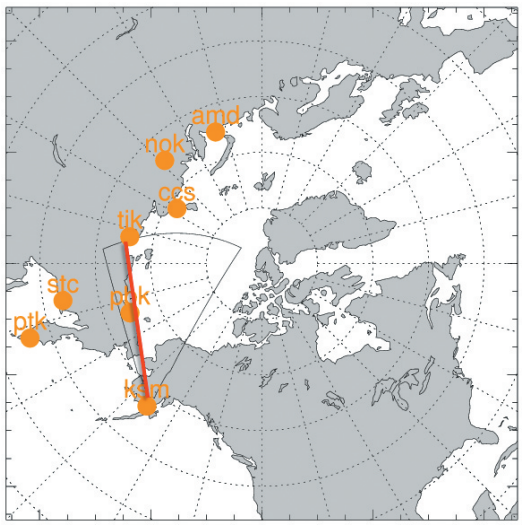

Fig.4 *KSR field of view at 09:00 hours UT on August 10, 2007*

This shows the locations of the King Salmon radar (KSR), NICT-SWM magnetometers, and RapidMag magnetometers. The red line denotes the location of the second beam of the KSR (Altitude Adjusted Corrected Geomagnetic Coordinates: AACGM coordinate system).

PBK and TIK (essentially facing westward), thereby enabling the monitoring of plasma velocity in the east-west direction near the magnetic latitudes of 62 to 64°.

The upper part of Fig. 5 shows fluctuations (using a color contour chart) in the plasma velocity observed along beam 02 in the line-of-sight direction at time 6–11 UT. In the vicinity of range gates 10–30 (from the east coast of Siberia to the air over the west coast of Alaska) from which effective echoes return, a greater proportion of the plotted time period appears from yellow to red, indicating dominance of the westward plasma flow apart from the radar, or as predicted from the average pattern of large-scale convections. Since the westward plasma flow was interrupted for about 10 minutes twice—once at ~08:10 UT and once at ~09:00 UT, with the contour appearing yellowish green—the direction of plasma flow is found reversed to face slightly eastward.

The diagram below depicts fluctuations in the H-component (horizontal northward com-

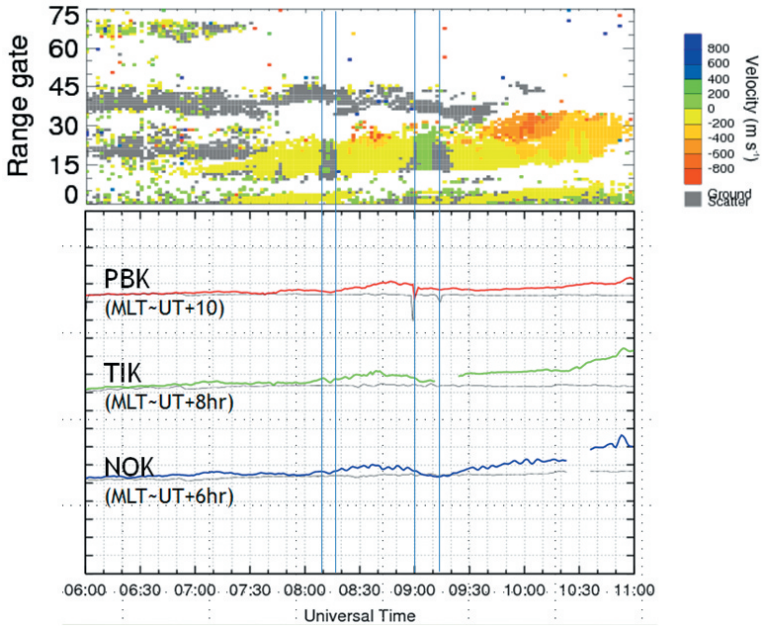

Fig.5 *Comparison of Doppler velocity observed on the KSR beam 2 and geomagnetic fluctuations*

Doppler velocity (upper diagram) heading towards the KSR has been observed twice (during time intervals enclosed by vertical lines), when DP2 current system decay is found from geomagnetic observations (lower diagram: 50 nT/div) at the same time.

ponent) of ground magnetic field observed by PBK, TIK and NOK at the same time. The continuous solid lines in red, green and blue in the diagram represent observed values at the same time (on August 10 of the same year) when extremely calm geomagnetic activities as represented in gray lines were observed. The appearance of very coherent fluctuations among three observatories varying in terms of local time apparently suggests that such geomagnetic fluctuations are due to DP2 current system fluctuations that represent large-scale convections. The H-component is sensed to essentially increase starting from 08:00 UT on this date, but begins to temporarily decrease at 08:10 and 09:00 UT. Because the increase in the H-component signifies an increase in eastward ionospheric current (assuming hall current, equivalent to westward plasma convections), or the development of the DP2 current system (large-scale convections), it does not contradict the observation of westward plasma flow. In addition, the eastward plasma flow mentioned above appears at the timing of decay in the DP2 current system, and if the eastward flow is assumed to represent decay of the westward flow, degradation of the DP2 current system, hence that of large-scale convections, may be manifested as a radar observation.

While the one-dimensional spatial structure of plasma flow observed along a specific beam in the radar has been presented above, the KSR can perform similar observations along another beam in the field of view to produce a velocity field in a latitude-longitude two-dimensional plane. Figure 6 shows time changes in this velocity field for which snapshots were taken every four minutes during a 36-minute period involving a time zone (09:00 to 09:15 UT) where a second appearance of eastward flow was witnessed. Obviously, the eastward flow shown in Fig. 5 on the west side from 21 h magnetic local time (MLT) and distributed on the lower-latitude side (lower than 64° latitude), was coupled with a continuation of the same westward flow as that appearing at the preceding and succeeding

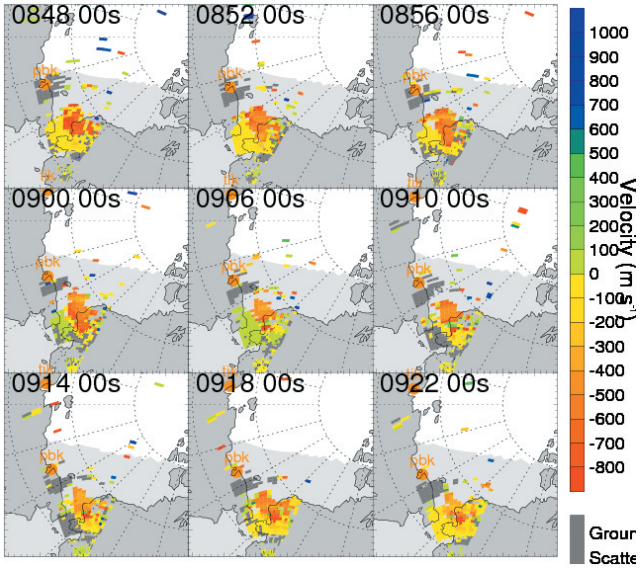

Fig.6 *Time-related changes in the two-dimensional plasma flow structure*

Two-dimensional structure of the ionospheric plasma flow observed by the KSR, and its temporal changes

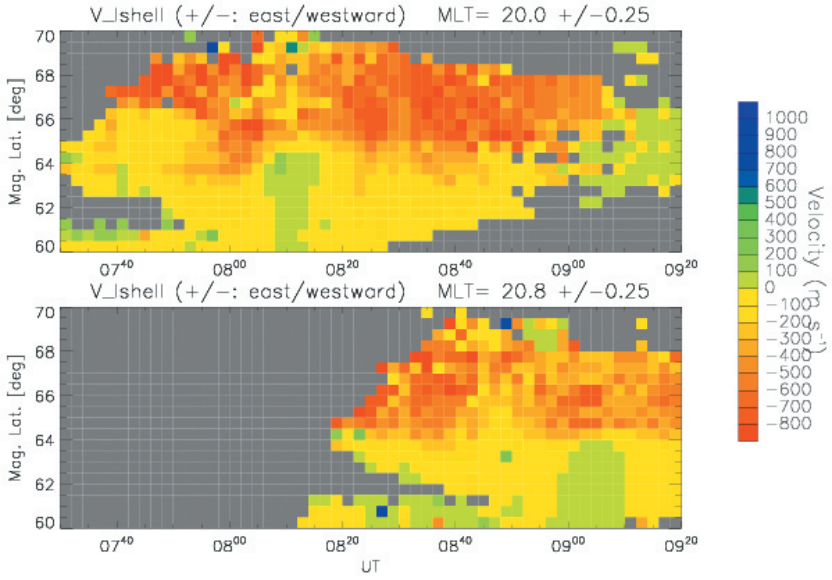

Fig.7 *Latitude structure of plasma flow velocity in the L-shell direction*

The latitude structure (upper diagram) of plasma drift velocity in the geomagnetic latitude direction (L-shell direction) produced by assuming that the Doppler velocity observed during a geomagnetic local time range of 20.0 h ± 0.25 h is the line-of-sight direction projection of plasma flow velocity in the geomagnetic latitude direction. Similar to the lower diagram, except that observations took place during a geomagnetic local time range of 20.8 h ± 0.25 h.

times on the higher-latitude side. Thus, flow shears that invoke westward flow on the higher-latitude side and eastward flow on the lower-latitude side have been formed.

Figure 7 shows the plasma flow observed in the line-of-sight direction as converted to

plasma flow velocity in the magnetic longitude direction (i.e., direction along the L-shell) to demonstrate the latitude dependence of velocity in the longitude direction, in an effort to gain detailed insight into the latitude structure of the flow shear. In this diagram, it is assumed that the velocity component of the actual plasma velocity existing in the longitude direction is projected in the line-of-sight direction to provide an actual radar view of the observed velocity. Thus, assuming that the actual plasma velocity and velocity projected in the line-of-sight direction are V_{Lshell} and V_{LOS}, respectively, and the angle formed by the line-of-sight direction of the beam with the longitude direction is θ, V_{Lshell} has been calculated by solving the equation:

$$V_{Lshell} = V_{LOS}/\cos\theta \quad (1)$$

The latitude structure of V_{Lshell} has been obtained from plasma velocities observed in the ranges of MLT = 20.0 h ± 0.25 h in the upper panel in Fig. 7 and MLT = 20.8 h ± 0.25 h in the lower panel. As can be understood from this diagram, the first flow shear formed at magnetic latitudes up to 64.5° at 08:05 to 08:15 UT, with the second flow shear appearing in the vicinity of magnetic latitude 64.0° at 08:58 to 09:15 UT. As flow shears are formed and extinguished, plasma flow varies from westward to eastward to westward on the lower-latitude side, but such reversals in velocity only take a few minutes. In terms of shear polarity and intensity, both shears form a westward flow at 300 to 500 m/s on the higher-latitude side and an eastward flow up to ~100 m/s on the lower-latitude side. The shear polarities apparently suggest a flow of downward field-aligned current (FAC). Because the earth's main magnetic field has a magnitude up to 60,000 nT in this vicinity according to the IGRF model, the poleward electric field at up to 24 mV/m on the higher-latitude side in this flow shear has changed to an equatorward electric field up to 3 mV/m on the lower-latitude side across the boundary of ~ only 1° in latitude, suggesting a steep spatial gradient in the electric field.

3 Statistical analyses

In the case study presented in the preceding chapter, the flow shear appearing on the evening side was formed at magnetic latitudes up to 64° at the timing of decay in the DP2 current system. Statistical analyses were then conducted to examine the extent to which such a result universally applies to other flow shears. First, all KSR data in effect from April 2007 to July 2008 were visually scanned to identify all instances of flow shears being confirmed between 15 h to 22 h MLT. In addition, when only those instances in which solar wind and IMF data were yielded from the ACE satellite concurrently with flow shear observation, and in which RapidMag geomagnetic data and THEMIS-GMAG geomagnetic data needed to grasp higher-latitude geomagnetic activities were available, a total of 26 instances of flow shear events was obtained during this period.

Figure 8 shows the locations of the 26 instances of flow shear events. Because the KSR field of view has a certain width in the MLT direction and flow shears are typically visible over a certain MLT width, the flow shear visible in each event is plotted as one polyline. As a result, flow shears have latitudes distributed between ~63 and 68° and

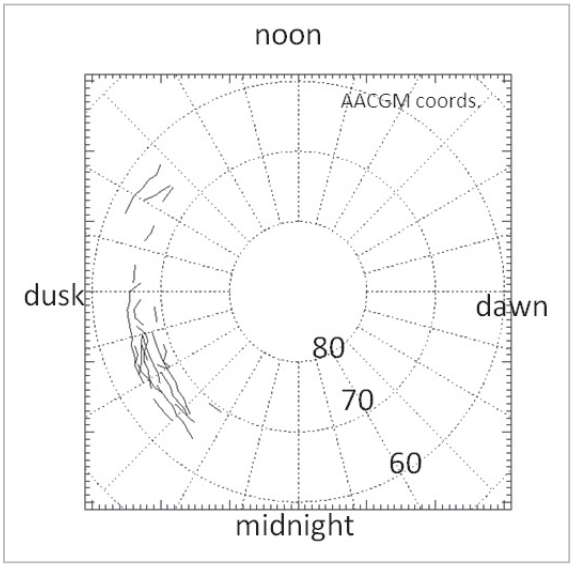

Fig.8 *Locations of flow shear observation*

most events are located at 18 h to 21 h MLT. Since such distributions are in virtual agreement with a range in which ionospheric echoes are easily observable, one can simply delineate a rough scope of distributions in the effective observation area of the KSR. Hence, this result does not exclude the possibility of flow shears having occurred outside the effective observation area.

Next, the geomagnetic activities that occurred concurrently with the flow shear events were identified with reference to RapidMag and THEMIS-GMAG geomagnetic data, along with the associated IMF fluctuations. Table 1 summarizes the results. One significant finding is that eight (up to 31 %) out of the 26 instances of flow shears had occurred in association with decay of the DP2 current system, when compared with double the occurrences (up to 62 %) during a substorm period, and not involving decay of the DP2 system. In seven of the eight instances of flow shears occurring at DP2 current system decay, a southward decrease in IMF or northward turn of IMF had occurred at the same time, which is not inconsistent with DP2 system decay. The instances of flow shears occurring during a substorm period showed no distinctive characteristics of IMF fluctuations. A probe into the substorm phase, though not presented here, located flow shears occurring at the onset of a substorm or during its expansion or recovery phase, thereby falling short of confirming the noticeable phase dependence of flow shears as being confined to a particular phase.

Those flow shear events characterized by precipitating particles concurrently observed by the NOAA/POES satellite (http://www.oso.noaa.gov/poes/) and Metop-2 satellite (http://www.esa.int/esaLP/LPmetop.html) were then extracted to examine the positional relationship between flow shears and the aurora oval. Because the precipitating particles distributed in the polar region have a complex spatial structure and involve marked time changes, our analyses focused only on those instances of flow sheers observed during the time zone in which the shears were observed by the KSR or during the preceding or succeeding five-minute period, and also observed by NOAA/POES or Metop-2 within the MLT range of their observation and within 0.5 h MLT from the east and west ends of the MLT range. Of all the 26 instances of flow sheer events, 12 yielded both extremely adjacent simultaneous observations spatially and timely. Figure 9 shows one such instance. The upper, middle and lower panels in the diagram represent the 30 to 80 keV ions, 30 keV and higher electrons, and the energy flux resulting from 20 keV and lower precipitating electrons observed by METOP-2 at 06:51 to 07:01 UT on April 5, 2007, respectively, when Metop-2p was orbiting at an altitude of about 850 km on the even side of the northern hemisphere (from the lower-latitude side to the higher-latitude side). As can be seen from the lower panel, the precipitating electron energy flux begins to show sharp advances starting from 06:56 UT, exceeding 0.1 erg/cm^2 · str · keV · sec at 06:56:30 UT (68°magnetic latitude, 18.3 h MLT) and an empirical flux level of 1.0 erg/cm^2 · str · keV · sec [7] needed to create a visible aurora at 06:58:30 UT (72° magnetic latitude, 17.4 h MLT). The satellite is assumed to have reached an altitude above the electron-

Table 1 *Correspondence between geomagnetic activities and IMF fluctuations upon the formation of flow shears*

A summary correspondence between the presence or absence of DP2 decay and substorms on the occurrence of flow shears, and IMF fluctuations

	IMF N-turning or SIMF decrease	IMF S-turning or SIMF increase	Unclear variation	TOTAL
DP2 decay	7	0	1	8
With substorm	2	2	12	16
(unclear)	0	0	2	2
TOTAL	9	2	15	26

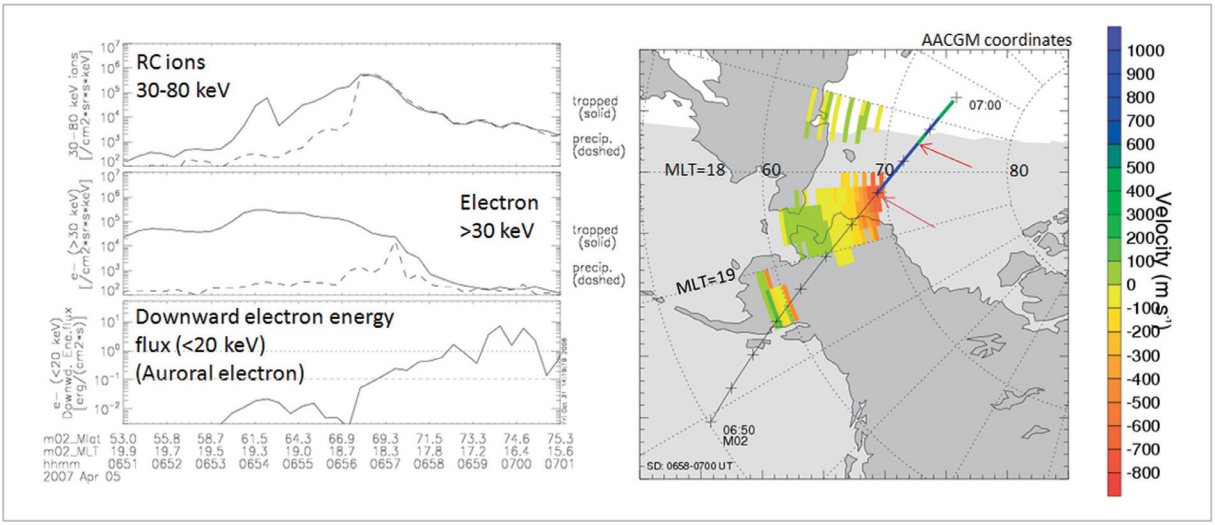

Fig.9 *Positional relationship between Metop-2 satellite aurora oval observations and flow shear location*

(Left diagram) Trapped and precipitating ions (upper panel) having energy of 30 to 80 keV observed by the Metop-2 satellite over Alaska at 06:51 to 07:01 UT on April 5, 2007, and trapped and precipitating electrons (middle panel) having energy of 30 keV or more and energy flux (lower panel) caused by precipitating electrons having energy of 20 keV or less (lower panel).

(Right diagram) The orbit of Metop-2 at this time. The red arrow denotes where the precipitating energy flux exceeds 0.1 (blue bold line) and 1.0 (green bold line) on the orbit [erg/cm^2 · str · ke · Esec] for the first time. Ionospheric plasma drift velocities in the L-shell direction observed by the KSR are represented in a color contour chart.

ic auroral oval in that vicinity (68 to 72° magnetic latitude). The diagram on the right shows the satellite orbit at this time and the flow shear observed at 06:58 to 07:00 UT. The flow shear was observed not only during this two-minute period, but all the time from 06:50 to 07:10 UT including that period. The aurora oval had an estimated low magnetic latitude boundary of 68° at the lowest, so the flow shear occurring in the vicinity of 65° is found to have been forced on the lower-latitude side of the auroral region, or in a subauroral region.

Such analyses were iterated for all 12 instances of flow sheers to develop the relationship between flow shear latitude and the low latitude boundary of the aurora oval as shown in Fig. 10. The results reveal that flow shears always formed in a subauroral region 1 to 6° lower in latitude than the aurora oval. According to comparisons with the ion isotropic boundary determined by the flux ratio of trapped and precipitating ions, though

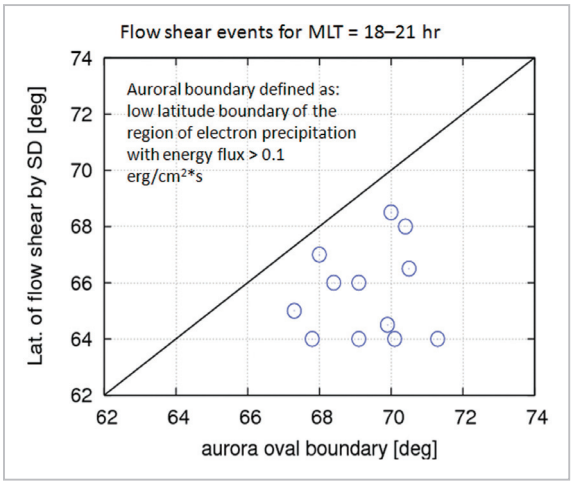

Fig.10 *Comparison of flow-shear latitude with lower-limit latitude of the aurora oval*

Comparisons of the latitude of flow shears with the low-latitude boundary location of the aurora oval observed by NOAA and Metop satellites

not presented in this paper, flow shears have been found to reside 2 to 3° lower in latitude than the 30 to 80 keV ionic isotropic boundary,

suggesting that flow shears have been formed in the region dominated by 30 to 80 keV trapped particles in a subauroral region.

4 Discussions

Flow shears on the evening observed this time can generally be perceived as a consequence of relative intensity changes in Region-1 field-aligned current (Region-1 FAC) and Region-2 field-aligned current (Region-2 FAC) [8]. Figure 11 shows a schematic view. In a situation where southward IMF intensifies similarly to magnetospheric convections (left in the diagram), FAC that generates an ionospheric electric field driving a clockwise convection vortex (orange arrow), or upward FAC (sensed in Region 1 on the evening side) is found to increase. Expanding convections allow particles to be injected into the inner magnetosphere on the night side, thereby forming a partial ring current (PRC) [9]. Since this PRC closes as a current, a downward FAC (sensed in Region 2, blue dotted arrow) should be produced in the lower-latitude region than that of FAC, but while the PRC has not yet fully grown, the clockwise convection vortex resulting from the upward FAC electric field excels, resulting in a westward flow (black arrow) in the auroral region to subauroral region on the evening side. But once the southward IMF that drives the convection weakens or turns northward (right in the diagram), the magnetic reconnection will rapidly degrade on the daytime magnetospheric boundary, possibly followed by rapid weakening of the upward FAC and clockwise convection vortex driven by an electric field generated by the upward FAC. Then, if the PRC has fully grown, the downward FAC produced by PRC generates a reverse electric field, resulting in a counterclockwise convection vortex (blue continuous solid arrow) being driven. A westward flow is consequently predicted to develop on the higher-latitude side of given latitude, with an eastward flow appearing on the lower-latitude side (black arrow). This precisely reflects the status of the ionospheric electric field and FAC at the time of DP2 current system decay, but from the standpoint of PRC-originated downward FAC (Region-2 FAC) gaining intensity relative to upward

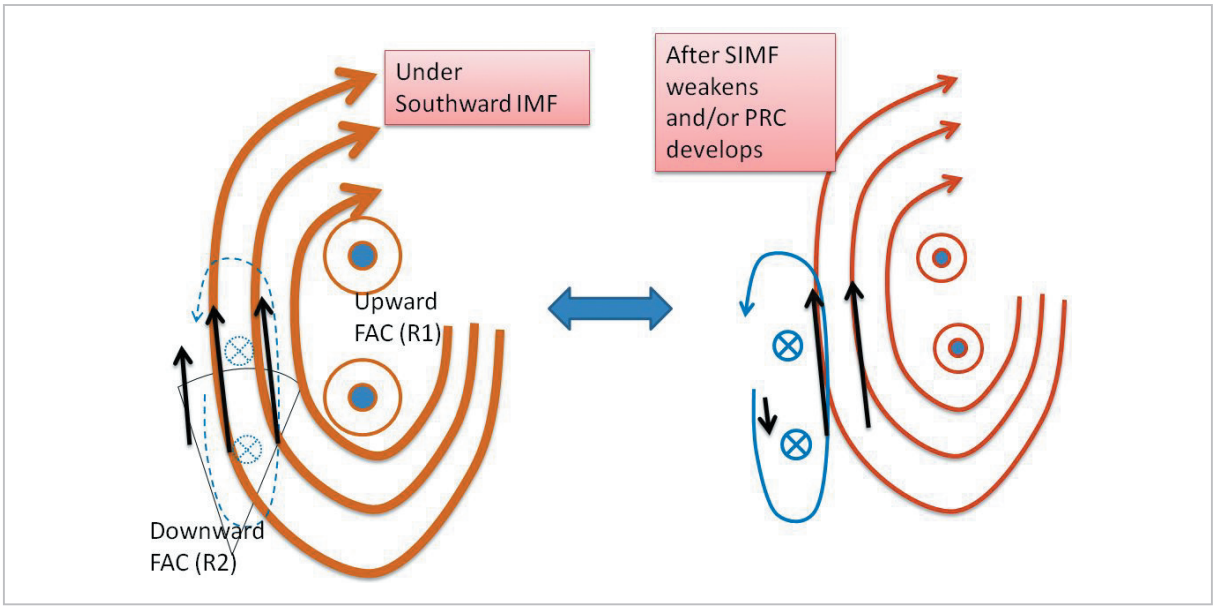

Fig.11 *Fluctuations in the balance of Region-1/Region-2 field-aligned currents and convection patterns*

Schematic diagram representing southward IMF fluctuations, and changes in the balance of the Region-1/Region-2 FAC-originated convection vortex associated with the growth of partial ring current (PRC)

FAC (Region-1 FAC), a similar condition is also assumed to be in effect during a substorm period (particularly after its onset). It may thus be concluded that flow shears observed at both decay of the DP2 current system and during a substorm period are the result of a transient intensification of Region-2 FAC relative to Region-1 FAC.

The intensifying Region-2 FAC as compared with Region-1 FAC, with a reverse electric field appearing on the lower-latitude side, is exactly the same as the overshielding observed during a magnetic storm or substorm period[10][11]. Ishikawa et al.[12] have conducted earlier studies on the subject of overshielding with reference to IMAGE geomagnetic chain data. The following presents a comparative discussion of the results of this research with such earlier studies.

Ishikawa et al.[12] defined that, while eastward current (or the H-component) pointing to DP2 current in the mid-latitude to auroral region on the afternoon to evening side increases, the H-component may change due to a reduction in mid-latitude across a certain point of time, and that such an event may suggest the presence of shielding (or overshielding), and also examined in detail to what latitude the reduction in the H-component is visible. Figure 12 plots the latitude at the high-latitude limit of H-component reduction superimposed with the latitude of flow shears observed in this research. Assuming that fluctuations in the ground magnetic field reflect those in hall current in the ionosphere directly above, the structure of eastward current being formed on the higher-latitude side and westward current on the lower-latitude side may have a direct bearing on westward ionospheric convections on the higher-latitude side and eastward ionospheric convections on the lower-latitude side. The boundary can be regarded as a boundary of contact with a region dominated by the electric field and current resulting from Region-1/Region-2 FAC at overshielding. Despite uncertainties about latitude differences from the magnetometer (where the H-component increases) directly adjoining the higher-latitude side, the work done by Ishikawa et al.[12] seems to be essentially in agreement with the flow shears observed in this research. Although identical flow shears should be located at the same latitudes, and against our expectations, the latitude of flow shears identified by the KSR is about 5° higher on average than the geomagnetically identified high-latitude limit of the westward current at overshielding. This is larger than the installation latitude intervals (up to about 2°) of the magnetometers mentioned earlier. There are also systematic differences in the Kp index on the statistical population of events between the work done by Ishikawa et al.[12] and this research, and such differences are clearly evident when comparing only the events with Kp = 2 common to both populations.

The latitude differences described above can be understood by allowing for fluctuations in the H-component caused by ionospheric current other than that existing directly above. Figure 13 summarizes the KSR observations at the formation of flow shears, the ionospher-

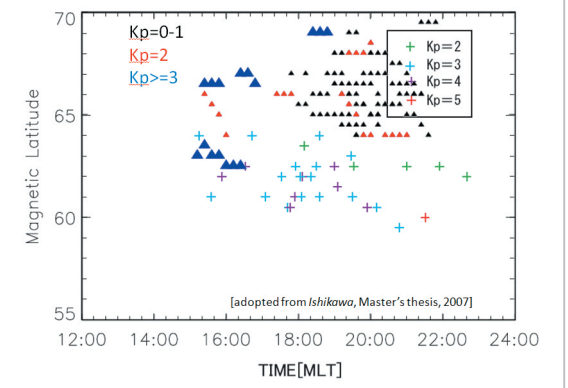

Fig.12 *Comparison of the high-latitude boundary of ionospheric westward current with flow sheer location*

Comparison of the location of (latitude, local time) of flow shears (triangle in the diagram) with the location (plus sign in the diagram) on the high-altitude boundary of ionospheric westward current determined from the IMAGE geomagnetic chain by Ishikawa et al.[11]. Marked in different colors according to KP index values at the same time.

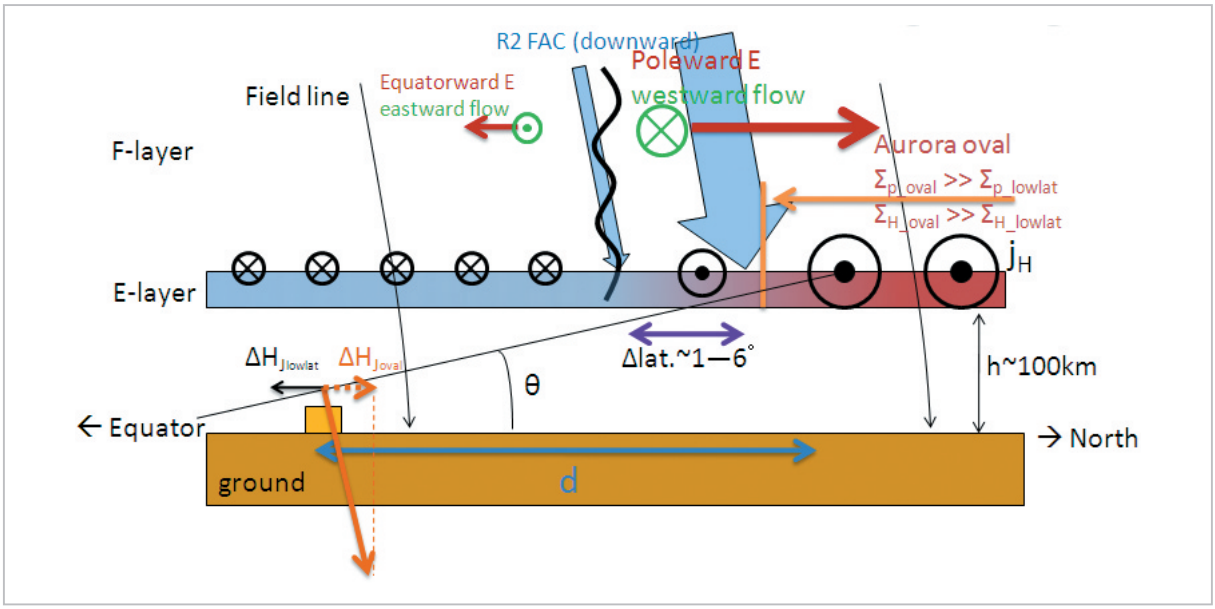

Fig. 13 *Relationship between ground magnetic field fluctuations and ionospheric current and field-aligned current, where ionospheric conductivity is not uniform*

Schematic diagram representing the ionospheric electric field and plasma convections, field-aligned current, and ionospheric hall current upon the formation of flow shears and variations in the H-component of the ground magnetic field formed thereof

ic current estimated therefrom, FAC and fluctuations appearing in the ground magnetic field to promote such understanding. Plasma flow (green mark in the diagram) moving westward or eastward on the higher- or lower-latitude side of a certain latitude, respectively, has been observed by the KSR, suggesting the presence of a poleward electric field (equator-ward electric field) on the higher-latitude side (lower-latitude side indicated by the red arrow). This electric field is imparted to the E-region along the field-aligned current to lead hall current (J_H) in the east-west direction. Based on these KSR observations, however, the electric field that drives the hall current is considered up to five times higher on the higher-latitude side than on the lower-latitude side, with hall conductivity of the auroral region on the higher-latitude side several to more than ten times higher than that of the lower-latitude side. As a result, the eastward current in the auroral region is estimated to be several tens of times higher than the westward current on the lower-latitude side. At a geomagnetic observation point (orange rectangle in the lower-left corner of the diagram) positioned in the subauroral region, the H-component fluctuations ($\Delta H_{Jlowlat}$) caused by ionospheric current directly above and the effect (ΔH_{Joval}) from current in a horizontally separate auroral region deserve notice. Because $\Delta H_{Jlowlat}$ and ΔH_{Joval} are opposed to each other, H-component variations apparently canceled at an observation point on a lower latitude than the boundary of the poleward and equator-ward electric fields (black undulating line); in other words, the boundary of east-west current determined from the geomagnetic H-component is expected to be located on the lower-latitude side rather than the boundary of the poleward and equator-ward electric fields, thereby showing good agreement with the findings shown in Fig. 12.

The actual extent to which the point of cancellation in H-component fluctuations (i.e., $\Delta H_{Joval} = \Delta H_{Jlowlat}$) is shifted towards a lower latitude ("d" in the diagram) can be estimated by using line current approximation to assess the effect of hall current in the ionosphere on the ground magnetic field.

$$\Delta H_{Jlowlat} \propto J_{H_{lowlat}}/h \quad (2)$$

$$\Delta H_{Joval} \propto J_{H_{oval}} \sin\theta/\sqrt{(d^2+h^2)} \quad (3)$$

where, $J_{Hlowlat}$ and J_{Hoval} denote the westward ionospheric hall current directly above the geomagnetic observation point and the eastward hall current in the auroral region, respectively, and h denotes the altitude (assumed at 100 km for now) of the E-region of the ionosphere. The magnitude of hall current is proportional to the product of hall conductivity Σ_H in the ionosphere and the magnitude of the poleward electric field Ep ($J_H \propto \Sigma_H \cdot E_p$). The ratio of the poleward electric field of flow shears on the higher-latitude side to their equator-ward electric field on the lower-latitude side has been typically found to be about five from the KSR observations in this research. Assuming that the ratio of Σ_H in the auroral oval to the subauroral region is about five to ten times, then one obtains a value of 25 to 50 for $J_{Hloval}/J_{Hlowlat}$. When this is applied to Equations (2) and (3), and assuming $\Delta H_{Jlowlat}/\Delta H_{Joval} = 1$, d is calculated to be 500 to 700 km. This distance is equivalent to a latitude width of 4.5 to 6.3° and is in good agreement with the latitude difference of 5° shown in Fig. 12. This finding should quantitatively support that the point of polar reversal in H-component fluctuations in the ground magnetic field gets shifted on the lower-latitude side by several degrees from the position of changes in ionospheric current directly above under the influence of high westward current at higher latitudes.

Next, we will discuss the relationship between the ionospheric plasma flow on the evening side (known from past studies) and the flow shears identified in this research. The findings shown in Fig. 10 indicate that the flow shears observed by the KSR had been formed in the subauroral region several degrees lower than the auroral oval. Fast (300 to 500 m/s) westward plasma flow exists on the higher-latitude side of the flow shears at this time, with the low-latitude portion of the westward flow also being positioned in the subauroral region. With flow shears formed during a substorm period in particular, one may be viewing the same thing as Subauroral Polarization Streams (SAPS) [13] from the standpoints of location (latitude, MLT) and magnitude of plasma flow velocity. A similar westward flow has actually been identified as SAPS or an Auroral Westward Flow Channel (AWFC) by the same KSR or another SuperDARN radar [14][15]. Therefore, the flow shears analyzed this time may well be an observational perception of the lower-latitude side of SAPS or AWFC.

There is no simple way to compare the central latitude and latitude width of SAPS indicated by *Foster and Vo* [13], because both have been calculated using Kp = 4 or more, which is different from the Kp level (Kp: 0 to 3) used for flow shear events in this research. However, a look at the statistical findings derived from Kp = 4 shows that the central latitude of SAPS at 18 h MLT is 63.5°, with the latitude width of SAPS at 22 h MLT averaging at about 3.5°. Therefore, it follows that the low latitude boundary of SAPS is about 60°. Flow shears treated in this research have an average latitude of 66°, which is higher than the low latitude boundary of SAPS. As Kp increases, however, the aurora oval and SAPS get shifted on the lower-latitude side by several degrees to 10° or more, suggesting that the differences fall into a fully conceivable range in both quantitative and qualitative terms. If statistical findings based on lower Kp values are yielded from ground radar or polar-orbiting satellite observations other than SuperDARN, a more detailed comparison might be possible.

5 Summary and conclusions

East-west flow shears formed on the evening side in the auroral region to the subauroral region of the ionosphere as observed by the King Salmon radar have been subjected to a case study and statistical analyses to draw the following conclusions:

• Flow shears found on the evening side are a

fast westward flow (~300 – 500 m/s) on the higher-latitude side and an eastward flow having a velocity of several tens to 100 m/s on the lower-latitude side, with the east-west plasma flow boundaries being distributed across magnetic latitudes of 63 to 68°.

- In addition to being formed at the timing of DP2 current system decay, flow shears tend to occur in the expansion and recovery phases associated with substorms.
- Flow shears on the higher-latitude side during a substorm period and fast westward plasma flow are associated with SAPS/AWFC, so the flow shears identified in this research can be considered to represent the structure of the lower-latitude side boundaries of SAPS/AWFC.
- The electric field associated with Region-1 may weaken at decay of the DP2 current system and PRC increases during a substorm period, resulting in the electric field structure and convex vortex associated with Region-2 FAC being intensified relative to those associated with Region-1 FAC, thereby accounting for the occurrence of such transient flow shears.

Acknowledgements

This research has been conducted with the aid of SuperDARN King Salmon radar data, NICT-SWM geomagnetic data, and RapidMag geomagnetic data furnished by the National Institute of Information and Communications Technology. The author wishes to thank Mr. Shinichi Watari and the administrators of SuperDARN, NICT-SWM and RapidMag. The ACE satellite data used in this research was downloaded from the ACE Science Center (http://www.srl.caltech.edu/ACE/ASC/).

References

1 Greenwald, R. A., K. B. Baker, J. R. Dundeney, M. Pinnock, T. B. Jones, E. C. Thomas, J. - P. Villain, J. - C. Cerisier, C. Senior, C. Hanuise, R. D. Hunsucker, G. Sofko, J. Koehler, E. Nielsen, R. Pellinen, A. D. M. Walker, N. Sato, and Y. Yamagishi, "DARN/SuperDARN, A global view of high-latitude convection," Space Sci. Rev., Vol. 71, pp. 763–796, 1995.

2 Baker, J. B. H., R. A. Greenwald, J. M. Ruohoniemi, K. Oksavik, J. W. Gjerloev, L. J. Paxton, and M. R. Hairston, "Observations of ionospheric convection from the Wallops SuperDARN radar at middle latitudes," J. Geophys. Res., Vol. 112, A01303, doi: 10.1029/2006JA011982, 2007.

3 Hashimoto, K. K., T. Kikuchi, M. Kunitake, K. Ohtaka, and S. Watari, "Ionospheric plasma convection observed by HF radar network in the northern polar region," Journal of the National Institute of Information and Communications Technology, Vol. 54, No. 1/2, pp. 103–111, 2007.

4 Nishida, A., N. Iwasaki, and T. Nagata, "The origin of fluctuations in the equatorial electrojet: a new type of geomagnetic variation," Ann. Geophys., Vol. 22, pp. 478, 1966.

5 Nishida, A., "Geomagnetic 2 fluctuations and associated magnetospheric phenomen," J. Geophys. Res., Vol. 73, pp. 1795–1803, 1968.

6 Kikuchi, T., K. K. Hashimoto, M. Shinohara, K. Nozaki, and B. Bristow, "Space weather study using the HF radar in King Salmon, Alaska," Journal of the National Institute of Information and Communications Technology, Vol. 54, No. 1/2, pp.113–121, 2007.

7 Yahnin, A. G, V. A. Sergeev, B. B. Gvozdevsky, S. Vennerstrom, "Magnetospheric source region of discrete auroras inferred from their relationship with isotropy boundaries of energetic Particles," Ann. Geophys., Vol. 15, pp. 943–958, 1997.

8 Iijima, T. and T. A. Potemra, "Large-scale characteristics of field-aligned currents associated with substorms," J. Geophys. Res., Vol. 83, pp. 599–615, 1978.

9 Hashimoto, K. K., T. Kikuchi, and Y. Ebihara, "Response of the magnetospheric convection to sudden interplanetary magnetic field changes as deduced from the evolution of partial ring currents," J. Geophys. Res., Vol. 107, No. A11, 1337, doi: 10.1029/2001JA009228, 2002.
10 Kikuchi, T., H. Luhr, K. Schlegel, H. Tachihara, M. Shinohara, and T. - I. Kitamura, "Penetration of auroral electric fields to the equator during a substorm," J. Geophys. Res., Vol. 105, No. A10, pp. 23,251–23,261, 2000.
11 Ebihara, Y., N. Nishitani, T. Kikuchi, T. Ogawa, K. Hosokawa, and M. - C. Fok, "Two-dimensional observations of overshielding during a magnetic storm by the Super Dual Auroral Network (SuperDARN) Hokkaido radar," J. Geophys. Res., Vol. 113, A01213, doi: 10.1029/2007JA012641, 2008.
12 Ishikawa, Y., K. K. Hashimoto, T. Kikuchi, T. Watanabe, M. Kunitake, and K. Ohtaka, "Overshielding of the convection electric field in the ionosphere," Journal of Kibi International University School of Policy Management, Vol. 3, pp. 31–41, 2007.
13 Foster, J. C. and H. B. Vo, "Average characteristics and activity dependence of the subauroral polarization stream," J. Geophys. Res., Vol. 107, No. A12, 1475, doi: 10.1029/2002JA009409, 2002.
14 Koustov, A. V., R. A. Drayton, R. A. Makarevich, K. A. McWilliams, J. - P. St-Maurice, T. Kikuchi, and H. U. Frey, "Observations of high-velocity SAPS-like flows with the King Salmon SuperDARN radar," Ann. Geophys., Vol. 24, pp. 1591–1608, 2006.
15 Parkinson, M. L., M. Pinnock, H. Ye, M. R. Hairston, J. C. Devlin, P. L. Dyson, R. J. Morris, and P. Ponomarenko, "On the lifetime and extent of an auroral westward flow channel (AWFC) observed during a magnetospheric substorm," Ann. Geophys., Vol. 21, pp. 893–913, 2003.

***HORI Tomoaki**, Dr. Sci.*
Assistant Professor, The Solar-Terrestrial Environment Laboratory, Nagoya University
Magnetosphere Physics